370 *Inorg. Chem.* **2000,** *39,* 370−374

Electronic Absorption and MCD Spectra for $Pt(AuPPh_3)_8^{2+}$ and $Au(AuPPh_3)_8^{3+}$ Cluster Complexes in Poly(methyl methacrylate) Thin Films at 295 and 10 K

W. Roy Mason

Department of Chemistry and Biochemistry, Northern Illinois University, DeKalb, Illinois 60115

Received September 13, 1999

Electronic absorption and 8 T magnetic circular dichroism (MCD) spectra are reported for nitrate salts of $Pt(AuPPh_3)_8^{2+}$ and $Au(AuPPh_3)_8^{3+}$ in poly(methyl methacrylate) (PMM) thin films at 295 and 10 K in the vis−UV region from 1.6 to 3.6 μm^{-1} ($1\ \mu m^{-1} = 10^4\ cm^{-1}$). Enhanced resolution is observed at low temperature, especially for $Pt(AuPPh_3)_8^{2+}$, which emphasizes the differences in the nature of the low-energy excited configurations and states between $Pt(AuPPh_3)_8^{2+}$ and $Au(AuPPh_3)_8^{3+}$. The absorption and MCD spectra for $Pt(AuPPh_3)_8^{2+}$ are interpreted in terms of a combination of excitations from filled Pt 5d orbitals to empty Au framework 6s orbitals and intraframework Au_8^{2+} (IF) transitions, whereas the spectra for $Au(AuPPh_3)_8^{3+}$ are ascribed entirely to Au IF transitions.

Introduction

Acetonitrile solution electronic absorption and magnetic circular dichroism (MCD) spectra for a variety of centered gold cluster complexes, including $M(AuPPh_3)_8^{2+}$, M = Pd or Pt (D_{4d} centered crown structure, **1**), and $Au(AuPPh_3)_8^{3+}$ (D_{2h} centered icosahedral fragment structure, **2**) were recently measured and interpreted.[1,2] These interesting strongly colored cluster complexes[3] have numerous absorption bands in the vis−UV region, but in general the absorption spectra are rather poorly resolved and tend to appear similar for different complexes. However, a significantly greater MCD intensity and complexity was observed among the lowest energy bands in the spectra for $Pt(AuPPh_3)_8^{2+}$ than found for related complexes such as $Pd(AuPPh_3)_8^{2+}$ or $Au(AuPPh_3)_8^{3+}$. The hypothesis was advanced[1] that the greater MCD intensity could be traced to low-energy transitions from 5d orbitals on the central Pt to the framework orbitals of the peripheral Au atoms, which were described as combinations of Au 6s orbitals. The greater MCD signals were attributed to greater magnetic moments resulting from the angular momentum of the Pt 5d orbitals. In contrast, the low-energy bands for the Pd- or Au-centered cluster complexes were assigned to intraframework (IF) transitions involving excitations from an occupied framework MO to low-energy empty framework orbitals on the peripheral Au atoms of the cluster.[1,2] The MCD signals from these transitions were expected to be weaker because the source of angular momentum was of necessity from two-centered interactions among the 6s orbitals of the eight peripheral Au atoms in the cluster since single-centered 6s orbitals have no angular momentum. The 5d orbitals on the central Au or the 4d orbitals on the central Pd were assumed to be too stable to be found among the frontier orbitals in these cluster complexes. Furthermore, when CO reacts with $Pt(AuPPh_3)_8^{2+}$ to form the Pt-bonded CO complex $Pt(CO)(AuPPh_3)_8^{2+}$, the MCD spectrum[1] for $Pt(CO)(AuPPh_3)_8^{2+}$ becomes much weaker and appears similar to that for $Pd(AuPPh_3)_8^{2+}$ or $Au(AuPPh_3)_8^{3+}$. The MCD spectral change between $Pt(AuPPh_3)_8^{2+}$ and $Pt(CO)(AuPPh_3)_8^{2+}$ was interpreted as due to a shift of the Pt 5d → Au 6s transitions to higher energy as a result of Pt−CO bonding.[1] This blue shift of the Pt 5d → Au 6s transitions then revealed underlying IF transitions and the characteristically weaker MCD signals at low energy for $Pt(CO)(AuPPh_3)_8^{2+}$.

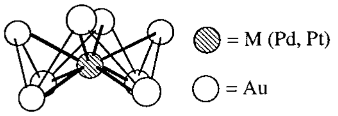

1

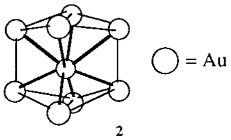

2

To further investigate the spectra for the $Pt(AuPPh_3)_8^{2+}$ and $Au(AuPPh_3)_8^{3+}$ cluster complexes and to reveal more of the details of the MCD spectral differences observed earlier in solution, some low-temperature (10 K) spectral measurements were made for nitrate salts of these complexes incorporated into thin poly(methyl methacrylate) (PMM) films. The PMM matrix, which preserves an isotropic solution-like environment for the complexes, was found to be transparent over the region of interest and could be cooled reversibly from 295 to 10 K without cracking or exhibiting excessive strain or birefringence. The low-temperature spectra described herein provide enhanced resolution and detail for further understanding of the low-energy excited configurations and states for $Pt(AuPPh_3)_8^{2+}$.

Experimental Section

Samples of $[Pt(AuPPh_3)_8](NO_3)_2$ and $[Au(AuPPh_3)_8](NO_3)_3$ were prepared as described earlier[1,2] and gave satisfactory elemental analysis and NMR spectra. The PMM films were prepared by dissolving a small amount of the solid nitrate salts in 3−5% PMM (Aldrich Chemical Co., average MW 120 000) dissolved in dichloromethane. The strongly colored red brown solutions were spread uniformly on microscope slides and allowed to evaporate slowly under a glass cover. During the evaporation, the samples were protected from exposure to light by

---

(1) Adrowski, M. J.; Mason, W. R. *Inorg. Chem.* **1997**, *36*, 1443. Adrowski, M. J. Dissertation, Northern Illinois University, 1996.

(2) Jaw, H.-R. C.; Mason, W. R. *Inorg. Cherm.* **1991**, *30*, 275.

(3) For a review of structures and reactions of gold cluster complexes, see: Pignolet, L. H.; Aubart, M. A.; Craighead, K. L.; Gould, R. A. T.; Krogsted, D. A.; Wiley, J. S. *Coord. Chem. Rev.* **1995**, *143*, 219. Mingos, D. M. P.; Watson, M. J. *Adv. Inorg. Chem.* **1992**, *39*, 327. Steggerda, J. J. *Comments Inorg. Chem.* **1990**, *11*, 113.

10.1021/ic991088o CCC: $19.00

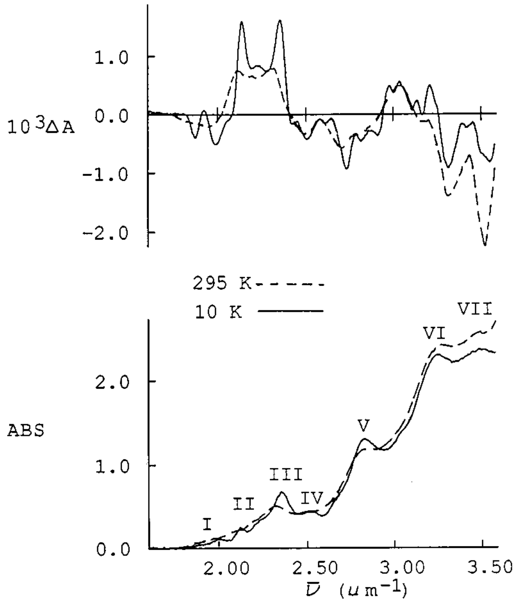

Figure 1. Absorption (lower curves) and MCD (upper curves) spectra for [Pt(AuPPh$_3$)$_8$](NO$_3$)$_2$ in a poly(methyl methacylate) thin film at 295 and 10 K. The *x*-axis units are 1 μm^{-1} = 10^4 cm^{-1}; the *y*-axis units are relative absorbance (ABS) and MCD differential absorbance (10$^3\Delta A$), respectively.

covering with aluminum foil. After 30 min to 1 h the solid films were hard and began to peal away from the glass slides; the films could be removed from the slides easily after a few hours further. Absorption spectra for these films taken over several days did not change. The film thickness, measured roughly by a sensitive caliper, was 30−50 μm, yet they were robust enough to be mounted in holders with tweezers. Films for measurements were selected to give absorbances between 0.0 and 2.5 in the region of interest.

Absorption spectra at room temperature were measured first on a Cary 5E spectrophotometer. Then simultaneous absorption and MCD spectra along a common light path were obtained at 295 and 10 K by means of a spectrometer described earlier,[4] together with a superconducing magnet system (Oxford Instruments Spectromag 4000) fitted with a variable temperature sample tube in which the sample was immersed in cooled He gas. The temperature was controlled to within 0.1 K. All reported spectra, both at 295 K and at 10 K, were corrected for a blank PMM film of comparable thickness but without the dissolved cluster complex. Each film that was cooled was recovered essentially unchanged upon rewarming to 295 K.

Results and Discussion

Figures 1 and 2 present the absorption and MCD spectra for Pt(AuPPh$_3$)$_8^{2+}$ and Au(AuPPh$_3$)$_8^{3+}$, respectively, in thin PMM films at 295 and 10 K. Numerical spectral data are collected in Table 1. The 295 K spectra in PMM for both cluster complexes are remarkably similar to the acetonitrile solution spectra reported earlier,[1,2] both in terms of band positions and relative band intensities. The greater MCD intensity in the low-energy region ($<$2.6 μm^{-1}) for Pt(AuPPh$_3$)$_8^{2+}$ compared to Au(AuPPh$_3$)$_8^{3+}$ is clearly evident. The 10 K PMM spectra show enhanced resolution of nearly all features for both cluster complexes, but the resolution for the MCD spectrum for Pt(AuPPh$_3$)$_8^{2+}$ in the interesting low-energy region is particularly enhanced. In fact the temperature dependence of this region for Pt(AuPPh$_3$)$_8^{2+}$ is distinctly greater than observed for Au(AuPPh$_3$)$_8^{3+}$, where the lowest bands are broad and show much less change upon cooling from 295 to 10 K. This observation tends to support the presence of different types of electronic transitions among the low-energy bands for the two cluster complexes as suggested earlier.[1]

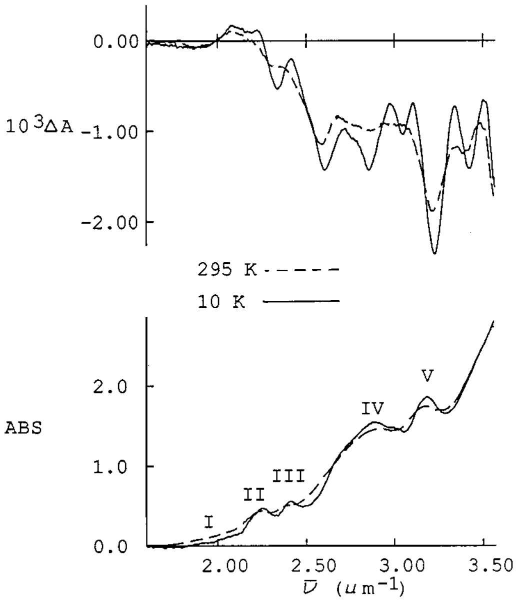

Figure 2. Absorption (lower curves) and MCD (upper curves) spectra for [Au(AuPPh$_3$)$_8$](NO$_3$)$_3$ in a poly(methyl methacylate) thin film at 295 and 10 K. Axis units are as in Figure 1.

Electronic States. Figure 3 presents a simplified energy level scheme showing the important one-electron MO's involved in the excited configurations, while Table 2 describes the one-electron cluster MO's for Pt(AuPPh$_3$)$_8^{2+}$, assuming D_{4d} symmetry for the PtAu$_8^{2+}$ framework, **1**. As described earlier,[1] the Au$_8^{2+}$ gold framework orbitals are composed of predominantly gold 6s valence orbitals containing a total of 6 electrons; the filled gold 5d orbitals are assumed to be too stable to participate in strong bonding, and the empty gold 6p orbitals are expected to be too high in energy to make a significant contributions to the framework orbitals. The Pt atom at the center of the cluster is assumed to be strongly bonded to the peripheral Au atoms through the empty Pt 6s orbital, and in the 16 valence electron cluster complex the platinum is formally 5d^{10}, Pt(0). The Pt(AuPPh$_3$)$_8^{2+}$ cluster complex is therefore diamagnetic with a 5d^{10}e$_1^4$ configuration, giving a ^{1}A$_1$ ground state. Table 3 gives the low-energy excited configurations and states based on the excitations visualized in Figure 3. The transitions between the occupied gold-based framework orbital e$_1$ to the empty framework MO's e$_2$, e$_3$, b$_2$, or 2a$_1$ are described as IF Au$_8^{2+}$ transitions, while the transitions involving excitation from the filled Pt(0) 5d orbitals are designated as Pt 5d → Au 6s in Table 3. Transitions in D_{4d} to B$_2$ (*z*-polarized) and E$_1$ (*xy*-polarized) states from the ^{1}A$_1$ ground state are dipole allowed; the degenerate E$_1$ states can exhibit both MCD *A* terms and *B* terms[5] while nondegenerate B$_2$ states can show only MCD *B* terms. Both zero-order singlet and triplet excited states expected in the absence of strong spin−orbit coupling and the relevant spin−orbit excited states are listed in Table 3, along with the sign of the MCD *A* terms previously determined for the E$_1$ states (see

---

(4) Mason, W. R. *Anal. Chem.* **1982**, *54*, 646. The spectrometer has been upgraded several times with some newer electronic components including a modern DSP lock-in amplifier (Stanford Research Instruments SR850), but the optical components and measurement methodology remain essentially the same.

(5) For a review of MCD term definitions together with the standard (Stephens) definitions and conventions that are used here, see: Piepho, S. B.; Schatz, P. N. *Group Theory in Spectroscopy with Applications to Magnetic Circular Dichroism;* Wiley-Interscience: New York, 1983.

Table 1. Spectral Data for Poly(methyl methacrylate) Thin Films

	295 K abs			295 K MCD			10 K abs			10 K MCD	
band no.	$\bar{\nu}$, μm^{-1}	λ, nm	A^a	$\bar{\nu}$, μm^{-1}	$10^3\Delta A^a$	band no.	$\bar{\nu}$, μm^{-1}	λ, nm	A^a	$\bar{\nu}$, μm^{-1}	$10^3\Delta A^a$
$[Pt(AuPPh_3)_8](NO_3)_2$											
				1.84	−0.17[b]	Ia	1.89	529	0.065[b]	1.87	−0.42
I	1.97	509	0.127[b]	1.94	−0.26					1.92	+0.06
						Ib	2.00	500	0.138	1.99	−0.53
										2.06	−0.12[b]
II	2.10	476	0.220[b]	2.11	+0.71	IIa	2.12	472	0.282	2.14	+1.57
						IIb	2.25	444	0.389[b]	2.23	+0.80
III	2.32	432	0.514	2.31	+0.73	III	2.36	425	0.713	2.35	+1.59
										2.42	−0.18
IV	2.51	399	0.454[b]	2.50	−0.39	IV	2.52	397	0.470	2.51	−0.45
										2.57	−0.11
										2.64	−0.10
				2.70	−0.63					2.74	−0.95
V	2.85	351	1.18	2.79	−0.39[b]	V	2.83	354	1.30	2.82	−0.49
										2.92	−0.38
										2.98	+0.46
VI	3.27	306	2.42	3.03	+0.43	VIa	3.04	3.29	1.39[b]	3.04	+0.53
				3.18	−0.18[b]					3.13	+0.20
						VIb	3.25	308	2.29	3.21	+0.47
				3.31	−1.44					3.31	−0.94
VII	3.48	287	2.73	3.52	−2.31	VII	3.49	286	2.36	3.55	−0.84
$[Au(AuPPh_3)_8](NO_3)_3$											
				1.87	−0.08	Ia	1.92	520	0.091[b]	1.88	−0.08
I	2.06	486	0.204[b]	2.08	+0.10	Ib	2.11	474	0.202	2.08	+0.17
II	2.25	445	0.462	2.33	−0.28[b]	II	2.25	444	0.521	2.22	+0.12
III	2.40	417	0.532[b]	2.58	−1.14	III	2.41	415	0.609	2.34	−0.54
										2.61	−1.42
IV	2.91	344	1.46	2.86	−0.99	IV	2.89	346	1.56	2.85	−1.42
										3.05	−1.03
V	3.18	315	1.74	3.21	−1.88	V	3.18	314	1.87	3.22	−2.35
				3.34	−1.17					3.34	−0.73
										3.42	−1.40
				3.49	−0.91					3.50	−0.66

[a] Relative values of absorbance (*A*) or differential absorbance (ΔA). [b] Shoulder.

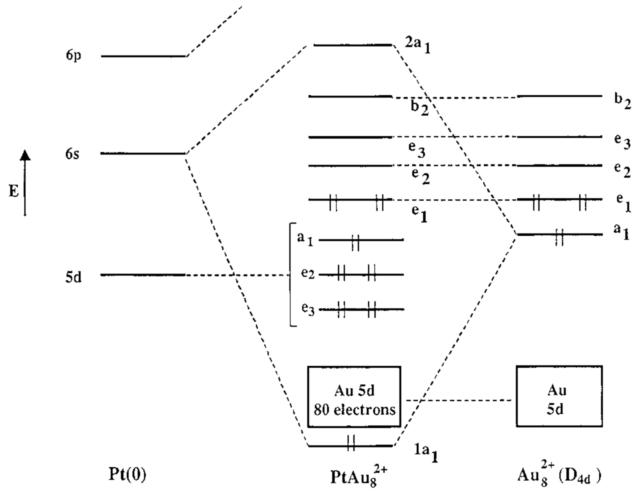

Figure 3. Simplified molecular orbital energy level scheme for $Pt(AuPPh_3)_8^{2+}$ assuming D_{4d} symmetry for the $PtAu_8^{2+}$ framework.

ref 1 for details of the *A* term sign determination). Although the structure **2** (D_{2h}) for the isoelectronic $Au(AuPPh_3)_8^{3+}$ complex is different from that of $Pt(AuPPh_3)_8^{2+}$, a D_{4d} structure similar to **1** is believed to be very close in energy and is even the observed structure in certain solid salts with related ligands bonded to the framework gold atoms (such as $(P(p\text{-}C_6H_4OMe)_3$ for example).[2,3] The cluster complex also has a 16 valence electrons, and the center Au may be viewed formally as $5d^{10}$, Au(I), but in contrast to $Pt(AuPPh_3)_8^{2+}$ the filled 5d orbitals on the center Au are believed to be too stable to be among the highest occupied MO's. The IF states for the diamagnetic D_{2h} complex have been described earlier[2] and are easily correlated with the IF states for D_{4d} given in Table 3.[1] Even though $Au(AuPPh_3)_8^{3+}$ may have a slightly different structure, its spectra are interpreted as due entirely to IF transitions[1,2] and thus the complex provides an important comparison case for interpreting the new features exhibited by $Pt(AuPPh_3)_8^{2+}$.

Table 2. One-Electron Molecular Orbitals for D_{4d} $PtAu_8^{2+}$

sym	energy[a]	MO wave function[b]
$1a_1^c$	$2\sqrt{2}\beta_1 + \beta_2$	$^1/_4(2\sqrt{2}\phi_1 + \phi_2 + \phi_3 + \phi_4 + \phi_5 + \phi_6 + \phi_7 + \phi_8 + \phi_9)$
e_1	$\sqrt{2}\beta_2$	$^1/_2\sqrt{2}(\sqrt{2}\phi_2 - \sqrt{2}\phi_4 + \phi_6 - \phi_7 - \phi_8 + \phi_9)$
		$^1/_2\sqrt{2}(-\sqrt{2}\phi_3 + \sqrt{2}\phi_5 - \phi_6 - \phi_7 + \phi_8 + \phi_9)$
e_2	0	$^1/_2(\phi_2 - \phi_3 + \phi_4 - \phi_5)$
		$^1/_2(\phi_6 - \phi_7 + \phi_8 - \phi_9)$
e_3	$-\sqrt{2}\beta_2$	$^1/_2\sqrt{2}(\sqrt{2}\phi_2 - \sqrt{2}\phi_4 - \phi_6 + \phi_7 + \phi_8 - \phi_9)$
		$^1/_2\sqrt{2}(-\sqrt{2}\phi_3 + \sqrt{2}\phi_5 + \phi_6 + \phi_7 - \phi_8 - \phi_9)$
b_2	$-2\beta_2$	$^1/_2\sqrt{2}(\phi_2 + \phi_3 + \phi_4 + \phi_5 - \phi_6 - \phi_7 - \phi_8 - \phi_9)$
$2a_1^c$	$-2\sqrt{2}\beta_1 + \beta_2$	$^1/_4(2\sqrt{2}\phi_1 - \phi_2 - \phi_3 - \phi_4 - \phi_5 - \phi_6 - \phi_7 - \phi_8 - \phi_9)$

[a] Hückel MO exchange integrals: β_1 from radial overlap of ϕ_1 with $\phi_2, \phi_3, \ldots \phi_9$; β_2 from adjacent tangential overlap ϕ_2, ϕ_9; ϕ_9, ϕ_5, etc.[b] ϕ_1 = Pt 6s orbital; ϕ_i = Au 6s orbital on atom *i* ($i > 1$). [c] For the hypothetical D_{4d} Au_8^{2+} cluster, this energy level is omitted and the energy of the a_1 becomes $+2\beta_2$ with ϕ_1 omitted from the $1a_1$ wave function.

Spectral Interpretation. As noted earlier, the general pattern of the absorption and MCD spectra at energies >2.6 μm^{-1} for $Pt(AuPPh_3)_8^{2+}$ (in the region of bands V−VII) and $Au(AuPPh_3)_8^{3+}$ (in the region of bands III−V) are similar, even though the MCD spectra for $Au(AuPPh_3)_8^{3+}$ show generally more negative signals. This higher energy region of the spectra for both complexes was interpreted[1,2] as due to IF transitions

Table 3. Low-Energy Excited Configurations and States for $Pt(AuPPh_3)_8^{2+}$

excited confgn[a]	zero-order states	spin−orbit states in D_{4d}[b]	*A* term sign[c]
		Intraframework (IF) Au_8^{2+}	
$e_1{}^3e_2$	$^1E_1$	$1E_1$	positive
	$^3E_1$	$2E_1$	positive
		$1B_2$	
		$(1B_1),(1E_2)$	
	$^1E_3$	$(1E_3)$	(positive)
	$^3E_3$	$(2E_3)$	(positive)
		$(1A_2)$	
		$(1A_1),(2E_2)$	
$e_1{}^3e_3$	$^1B_1$	$(2B_1)$	
	$^3B_1$	$3E_1$	positive
		$2B_2$	
	$^1B_2$	$3B_2$	
	$^3B_2$	$4E_1$	positive
		$(3B_1)$	
	$^1E_2$	$(3E_2)$	
	$^3E_2$	$5E_1$	∼0
		$(3E_3),(4E_2)$	
$e_1{}^3b_2$	$^1E_3$	$(4E_3)$	(negative)
	$^3E_3$	$(5E_3)$	(negative)
		$(2A_2)$	
		$(2A_1),(5E_2)$	
$e_1{}^32a_1$	$^1E_1$	$6E_1$	negative
	$^3E_1$	$7E_1$	negative
		$4B_2$	
		$(4B_1),(6E_2)$	
		Pt 5d → Au 6s[d]	
$a_1(Pt)e_2$	$^1E_2$	$(7E_2)$	
	$^3E_2$	$8E_1$	negative
		$(6E_3)$	(negative)
		$(8E_2)$	
$e_2(Pt)^3e_2$	$^1A_1$	$(3A_1)$	
	$^3A_1$	$(7E_3)$	(positive)
		$(3A_2)$	
	$^1A_2$	$(4A_2)$	
	$^3A_2$	$(8E_3)$	(positive)
		$(4A_1)$	
	$^1B_1$	$(5B_1)$	
	$^3B_1$	$9E_1$	positive
		$5B_2$	
	$^1B_2$	$6B_2$	
	$^3B_2$	$10E_1$	positive
		$(6B_1)$	
$e_3(Pt)^3e_2$	$^1E_1$	$11E_1$	positive
	$^3E_1$	$12E_1$	positive
		$7B_2$	
		$(7B_1),(9E_2)$	
	$^1E_3$	$(9E_3)$	(negative)
	$^3E_3$	$(10E_3)$	(negative)
		$(5A_2)$	
		$(5A_1),(10E_2)$	

[a] Filled orbitals omitted; notation as in Figure 3. Ground-state configuration: ... $e_1{}^4$ $^1A_1$. [b] Electric-dipole forbidden states in parentheses. [c] Estimated from eq 1 in ref 1 for E_1 states; for forbidden E_3 states (in parentheses), a distortion to a lower symmetry D_4 is assumed which gives allowed E states, for which the sign was estimated (see ref 1 for details). [d] $a_1(Pt)$ = Pt $5d_{z^2}$, $e_3(Pt)$ = Pt $5d_{xz}$, $5d_{yz}$, $e_2(Pt)$ = Pt $5d_{xy}$, $5d_{x^2-y^2}$.

based on the peripheral gold atoms. The low-temperature spectra show some enhanced resolution in both cases, but the basic pattern of bands in both absorption and MCD is unchanged. Therefore the previous IF interpretation seems appropriate and will not be reiterated here. The strong absorptions at energies >3.7 μm^{-1} for both cluster complexes are due to the PMM matrix and the PPh_3 ligands, and this region was not explored due to experimental limitations.

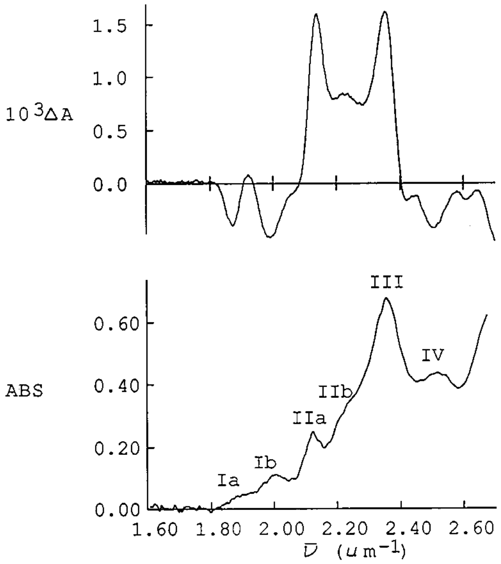

Figure 4. Expanded low-energy region of the 10 K absorption (lower curve) and MCD (upper curve) spectra for $Pt(AuPPh_3)_8^{2+}$. Units are as in Figure 1.

The more interesting region of the spectra is at low energy (<2.6 μm^{-1}), where the pattern in the MCD spectra for $Pt(AuPPh_3)_8^{2+}$ and $Au(AuPPh_3)_8^{3+}$ is remarkably different. The 10 K MCD spectra show an even greater difference between the two complexes in this region. Therefore, the discussion here will center on the interpretation of the features revealed in the 10 K $Pt(AuPPh_3)_8^{2+}$ spectra which is shown expanded in Figure 4. Bands I and II for $Au(AuPPh_3)_8^{3+}$ were assigned[2] as IF transitions, and as such they provide useful intensity comparisons for bands I−IV for $Pt(AuPPh_3)_8^{2+}$, which are attributed to a combination of both IF and Pt 5d → Au 6s transitions. The much greater intensity for the MCD signals in the $Pt(AuPPh_3)_8^{2+}$ spectrum compared to those for $Au(AuPPh_3)_8^{3+}$ (relative signals in the 10 K spectrum for $Pt(AuPPh_3)_8^{2+}$, for example, compared to those in the 10 K spectrum for $Au(AuPPh_3)_8^{3+}$ are greater by factors of 5−9; see Table 1) was interpreted earlier[1] as due to the presence of low-energy Pt 5d → Au 6s excitations. Both cluster complexes are expected to have similar IF transitions at low energy since the IF excitations are visualized as localized on the peripheral Au atoms and are expected to be more or less insensitive to the nature of the central atom in the complex.

The prominent and intense features in the low-energy MCD spectrum for $Pt(AuPPh_3)_8^{2+}$ (Figure 4) which correspond to bands Ia, Ib, IIa, and III are clearly different from any of the low-energy features in the MCD spectrum of $Au(AuPPh_3)_8^{3+}$ (Figure 2) and therefore are logically assigned to several Pt 5d → Au 6s transitions.. The three lowest energy MCD features appear to be overlapping positive *A* terms for bands Ia, Ib, and IIa, but the absorption band III (maximum at 2.355 μm^{-1}) is associated with a strong positive MCD signal (maximum at 2.353 μm^{-1}) at the same energy which is interpreted as a *B* term. The greater MCD intensity for bands IIa and III is ascribed to transitions to the predominantly singlet Pt 5d → Au 6s states $11E_1(^1E_1)$ and $6B_2(^1B_2)$ of the $e_3(Pt)^3e_2$ and $e_2(Pt)^3e_2$ excited configurations, respectively (see Table 3 for the notation for configuration and states). The positive *A* term observed for band IIa is consistent with the positive *A* term expected for $11E_1$, and the *B* term for band III is consistent with the nondegenerate $6B_2$ excited state. The unsymmetrical appearance of the *A* term for band IIa and the congested appearance of the MCD spectrum for bands Ia and Ib suggests the presence of weaker transitions to several states at similar energies. The predominantly triplet states of the $e_3(Pt)^3e_2$ and $e_2(Pt)^3e_2$ excited configurations are reasonable possibilities. For example, the $e_2(Pt)^3e_2$ states $10E_1$-

($^3B_2$), 9E_1($^3B_1$), and 5B_2($^3B_1$) are all expected to be lower in energy than 6B_2($^1B_2$) (band III). The positive *A* term for band Ib and the unsymmetrical appearance of the *A* term for band IIa may result from a superposition of the positive *A* terms predicted for the 10E_1 and 9E_1 states and the *B* term for the nondegenerate 5B_2 state. Similarly the $e_3(Pt)^3e_2$ states 12E_1($^3E_1$) and 7B_2($^3E_1$) states would be expected lower in energy than 11E_1($^1E_1$) (band IIa) in the region of band Ia. The positive *A* term expected for a transition to 12E_1 is consistent with the observed *A* term and the presence of a *B* term for the nondegenerate 7B_2 state may explain the unsymmetrical appearance of the lowest energy MCD feature. In contrast to these relatively intense MCD signals, the broad shoulder absorption band IIb has a corresponding MCD signal that is weaker and of uncertain term assignment between the strong MCD signals for bands IIa and III and thus is more similar to the weaker MCD signals observed for $Au(AuPPh_3)_8^{3+}$ at similar energies. Therefore consistent with earlier assignments[1,2] for both $Pt(AuPPh_3)_8^{2+}$ and $Au(AuPPh_3)_8^{3+}$ band IIb is assigned as the transition to the 1E_1($^1E_1$) state of the lowest energy IF configuration $e_1{}^3e_2$; the positive *A* term expected for this transition is likely partially obscured by the stronger MCD features for bands IIa and III. If this assignment is correct, then the corresponding predominantly triplet IF states of the $e_1{}^3e_2$ configuration, 2E_1($^3E_1$) and 1B_2($^3E_1$), are expected at lower energy than band IIb. However the positive *A* term and *B* term for these states, respectively, are expected to be weaker and therefore likely obscured by the more intense MCD for the Pt 5d → Au 6s transitions believed to be in the same energy region. It seems clear from this discussion that, even at 10 K, the MCD and absorption spectra for $Pt(AuPPh_3)_8^{2+}$ are not completely resolved, and several allowed states lie very close together in this low-energy region of the spectra, which causes the MCD spectra to exhibit overlapping and rather unsymmetrical *A* and *B* terms. Finally at higher energy the weaker negative MCD signal in the region of band IV (minimum at 2.51 μm^{-1}) corresponding to a broad resolved absorption at 10 K (maximum at 2.52 μm^{-1}) suggests a negative *B* term and therefore a transition to a nondegenerate state. A reasonable possibilitiy for band IV is the transition to the 2B_2($^3B_1$) state, a predominantly triplet state from the next lowest energy excited IF configuration $e_1{}^3e_3$. As noted earlier the higher energy region $>$2.6 μm^{-1} is dominated by IF transitions, but higher energy Pt 5d → Au 6s transitions are probably present in this region for $Pt(AuPPh_3)_8^{2+}$ as well and may contribute to some of the increased complexity observed, especially in the MCD, at 10 K.

Concluding Remarks. The experimental MCD spectra for $Pt(AuPPh_3)_8^{2+}$ are interpreted in terms of Pt 5d → Au 6s transitions at low energies among the IF transitions analogous to those found for $Au(AuPPh_3)_8^{3+}$. This interpretation is consistent with the Pt 5d orbitals being among the highest occupied orbitals in the cluster complex and embedded among the framework Au 6s orbitals. If the assignments given above are correct, then it may be noted that the Pt 5d → Au 6s transitions involve states from two different excited configurations, $e_2(Pt)^3e_2$ and $e_3(Pt)^3e_2$, in the same energy range, which in turn suggests that, apart from small differences in electron repulsions, the e_2(Pt) and e_3(Pt) orbitals have rather similar energies. The energy of the a_1(Pt) orbital is also likely similar, but states of the $a_1(Pt)e_2$ configuration were not specifically identified; the allowed (predominantly triplet) states of the $a_1(Pt)e_2$ configuration (see Table 3) predict only negative *A* terms in the MCD, but none were observed. The similarity of the energies of the Pt 5d orbitals suggests very weak "ligand field" effects from the surrounding peripheral Au atoms and is consistent with the view that these orbitals are essentially nonbonding and localized on the Pt atom in the center of the cluster complex. Consequently the Pt 5d orbitals would be exposed along the 4-fold axis of the D_{4d} structure where they would provide electron density in that direction. This feature may help explain why the $Pt(AuPPh_3)_8^{2+}$ complex is more reactive[3] to the addition of electrophilic reagents (CO, H_2, D_2, CN−R, Hg(0), −HgCl, etc.) than is $Au(AuPPh_3)_8^{3+}$. Such electrophiles would be attracted to the accessible 5d electron density of the Pt(0) center in the cluster complex.

IC991088O